ELSEVIER

Design of Concrete Mixes for Minimum Brittleness

D. Lange-Kornbak and B.L. Karihaloo
School of Civil and Mining Engineering, University of Sydney, Australia

Designers of concrete mixes are often faced with competing requirements such as high strength and high ductility and have to rely on empirical and heuristic approaches. In the present study, this is overcome by incorporating the characteristic length l_{ch} and the brittleness number B into the design criteria and using well-established, mostly nonempirical, formulae relating the effective properties (elastic modulus, tensile strength, and fracture energy) to the microstructural parameters (water/cement ratio, aggregate size, and volume fractions of coarse and fine aggregates). Nonlinear mathematical optimization problems, equivalent to the design criteria, are formulated and solved with a view to: (1) maximizing l_{ch} for a prescribed minimum direct tensile strength f'_t; (2) maximizing l_{ch} and f'_t simultaneously for a prescribed compressive strength f'_c; (3) minimizing B for a prescribed f'_c. ADVANCED CEMENT BASED MATERIALS, 1996, 3, 124–132

KEY WORDS: Brittleness number, Characteristic length, Fracture mechanics, Micromechanics, Microstructural parameters

Traditional concrete mix design is based on a compressive strength criterion often in combination with a workability criterion. Such an approach, however, ignores the importance of the intrinsic brittleness, that is, brittleness of the material, in governing the behavior (e.g., the bearing capacity) of structural concrete. This drawback can be met by using the fictitious crack model (FCM) [1,2], the size effect model [3], or the two-parameter model [4], as each provides a measure of the intrinsic brittleness. (For an overview, see ref 5.) Particularly the characteristic length of FCM has been successfully adopted in the design of new concrete materials, for example, by providing a microstructural brittleness number (B) useful in designing against microcracking [6]. This study, on the other hand, will demonstrate the application of FCM to conventional mixes. Such mixes allow a nonheuristic and, to a large extent, nonempirical microstructural design relying on known relationships between the microstructural parameters (geometrical and physical properties of the mix constituents) and the macroscopic response parameters (elastic modulus, tensile strength, and fracture energy). Thus, by formulating the design criteria as nonlinear mathematical optimization problems, optimum combinations of the water/cement (w/c) ratio, aggregate size, and volume fractions of coarse and fine aggregate can be obtained. In the present study, this is accomplished with a view to: (1) maximizing the characteristic length l_{ch} for a prescribed minimum direct tensile strength f'_t; (2) maximizing l_{ch} and f'_t simultaneously for a prescribed compressive strength f'_c; (3) minimizing B for a prescribed f'_c. The latter is desirable in order to reduce the extent of microcracking.

Micromechanical Relations

The characteristic length is defined in terms of the modulus of elasticity, E, the fracture energy, G_F, and the direct tensile strength, f'_t, by [1]

$$l_{ch} = \frac{EG_F}{f'^2_t}. \tag{1}$$

Micromechanical relations for these properties, as well as the uniaxial compressive strength f'_c, are presented in what follows.

Fracture mechanics permits the establishment of tension-softening relation $\sigma(w)$ or $w(\sigma)$ from which one can calculate the fracture energy [7]. Thus, micromechanical relations for G_F have been developed by Karihaloo [8], and Huang and Li [9]. The latter authors constructed the tension-softening curve from two separate curves (illustrated in Figure 1), the second part of the resulting curve being valid during frictional pull-out of the aggregates, $0 \leq \sigma \leq \sigma_f$. This leads to

$$G_F = \int_{\sigma=\sigma_f}^{f'_t} w(\sigma)d\sigma + \int_{\sigma=0}^{\sigma_f} w(\sigma)d\sigma = G_F^{(1)} + G_F^{(2)} \tag{2}$$

Address correspondence to: Dr. B.L. Karihaloo, School of Civil and Mining Engineering, University of Sydney, Sydney NSW 2006, Australia.
Received June 30, 1995; Accepted January 8, 1996

ISSN 1065-7355/96/$15.00
PII S1065-7355(96)00021-1

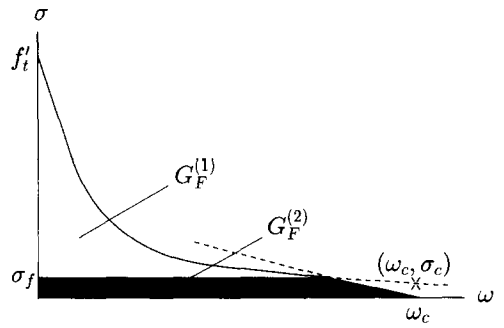

FIGURE 1. A typical tension-softening curve of concrete (after Huang & Li [7]).

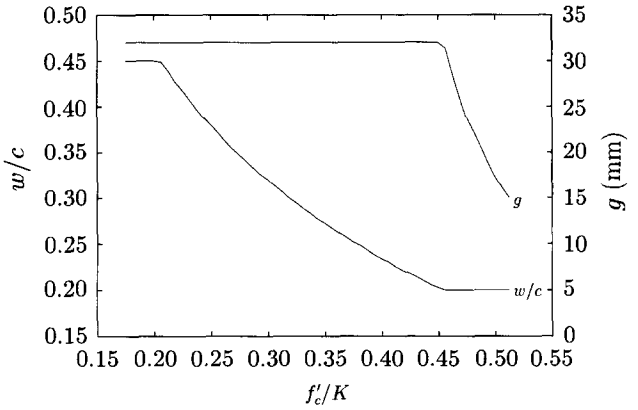

FIGURE 2. Optimum water/cement ratio and aggregate size versus relative compressive strength.

where

$$G_F^{(1)} = \frac{(K_{Ic})^2(1-\nu^2)}{E(1-V_{agg})} \times \left\{ \frac{1}{3}\left[\left(\frac{K_f}{\sqrt{2/\pi}K_{Ic}} \right)^3 - 1 \right] - \ln\left(\frac{K_f}{\sqrt{2/\pi}K_{Ic}} \right) \right\} \tag{3}$$

$$G_F^{(2)} = \int_{\sigma=0}^{\sigma_f} \left(\sqrt{\eta g} - \frac{g}{3\tau^* V_{agg}} \sigma \right) d\sigma$$

$$= \sqrt{\eta} K_f - K_f^2/(6\tau^* V_{agg}).$$

(In ref 9, the above exact solution to $G_F^{(1)}$ is not reported and $G_F^{(2)}$ is neglected.) ν is effective Poisson's ratio, E is effective modulus of elasticity, K_{Ic} is effective fracture toughness, η is surface texture parameter of the aggregate with the dimension of length, τ is shear strength of the aggregate–matrix interface, g is maximum size (diameter) of the aggregate, and V_{agg} is the total volume fraction of aggregates. $K_f = \sqrt{g}\sigma_f$ has been introduced and corresponds to the highest value of σ at which the tension-softening curves intersect, provided $\sigma_f \in [\sigma_c, f'_t]$. σ_c (actually $K_c = \sqrt{g}\sigma_c$) follows from the first part of the tension-softening curve by letting $\omega = \omega_c = \sqrt{\eta g}$. If a solution is lacking, $K_f = K_c$ is assumed, whereby $G_F = G_F^{(1)} + \sqrt{\eta} K_c$.

The application of fracture mechanics has also been illustrated by Karihaloo [8], Huang and Li [9], and Karihaloo et al. [10] on the example of macroscopic (measurable) uniaxial tensile strength. This property can be related to the maximum aggregate size through [9]

$$f'_t = \frac{K_{Ic}}{\sqrt{\pi g/2}}. \tag{4}$$

To complete the above formulae, an expression for the fracture toughness, K_{Ic}, is required. K_{Ic} depends on the operative toughening mechanisms. Thus, the toughening induced by crack deflection [9], distributed interfacial cracking [9], and bridging and trapping [11] over and above the matrix toughness, K_{Ic}^m, is given, respectively, by

$$\frac{K_{Ic}}{K_{Ic}^m} = \sqrt{1.0 + 0.87V} \tag{5}$$

$$\frac{K_{Ic}}{K_{Ic}^m} = \sqrt{\frac{1}{1-(\pi^2/16)V(1-\nu^2)}} \tag{6}$$

$$\frac{K_{Ic}}{K_{Ic}^m} = \sqrt{\zeta^2 + \frac{E(\pi/2)f_{t,a}^2 g_{av} V(1-\sqrt{V})(1-V)(1-\nu_m^2)}{E_m(1-\nu^2)(K_{Ic}^m)^2}} \tag{7}$$

where

$$\zeta = \left\{ 1 - \frac{(1-V)\pi/4}{\ln\{[1+\cos(\pi V/2)]/[\sin(\pi V/2)]\}} \right\}^{-1}$$

$$\frac{E}{E_m} = 1 - \frac{\pi^2}{16}(1-\nu^2)V$$

The relationship between E and the modulus of elasticity of the matrix, E_m, applies for $\nu = \nu_m$, where ν_m is Poisson's ratio of the matrix [9]. The parameter ζ takes the value 1 when the crack trapping mechanism is absent. In the above expressions, $f_{t,a}$ is the uniaxial tensile strength of the aggregate and g_{av} is the average aggregate size (diameter). For mortar, the matrix toughness K_{Ic}^m would equal that of the cement paste K_{Ic}^p, and V would be the volume fraction of the fine aggregate V_f;

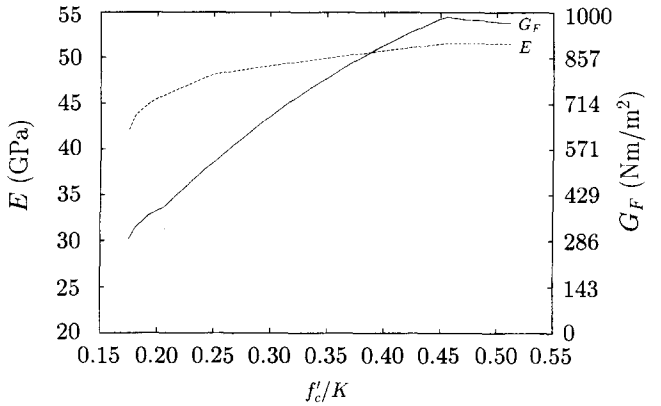

FIGURE 3. Optimum modulus of elasticity and fracture energy versus relative compressive strength.

whereas for concrete, K_{Ic}^m would be the fracture toughness of mortar, and V the volume fraction of coarse aggregate V_c. The fracture toughness of cement paste can be established from the experimental evidence gathered by Naus and Lott [12] and Ohgishi et al. [13], whereby

$$K_{Ic}^p = 0.6125 - 0.85\ w/c\ \text{MPa}\sqrt{\text{m}} \tag{8}$$

for $0.2 \leq w/c \leq 0.45$.

The effective fracture toughness resulting from any combination of the above mechanisms may now be constructed by simple multiplication of the respective toughening ratios, K_{Ic}/K_{Ic}^m, provided the mechanisms operate independently. In the present analysis, the fracture toughness of mortar is enhanced by bridging, crack deflection, and crack trapping, while that of concrete is further enhanced by bridging, deflection, and interfacial cracking.

For the determination of the modulus of elasticity, a method specially developed by Nielsen [14] for concrete is employed. Cement paste, mortar, and concrete are regarded as two-phase systems with the modulus of elasticity given by

$$E = E_m \frac{n + \Theta + V\Theta(n-1)}{n + \Theta - V(n-1)} \tag{9}$$

where V is the volume fraction of the discrete phase, Θ is a geometry function accounting for the configuration of the discrete phase, and n is the ratio of modulus of elasticity of the discrete phase to modulus of elasticity of the continuous phase, E_m.

For cement paste ($E = E_p$), a distinction is made between w/c ratios below and above $1.2\rho_w/\rho_c$ (ρ_w = density of water; ρ_c = density of unhydrated cement particles). In the former range, the cement paste is considered as a collection of unhydrated cement particles with modulus of elasticity E_u embedded in solid, hydrated cement gel with $E_m = 27200h$, where h is the degree of hydration. The volume fraction of unhydrated cement particles is

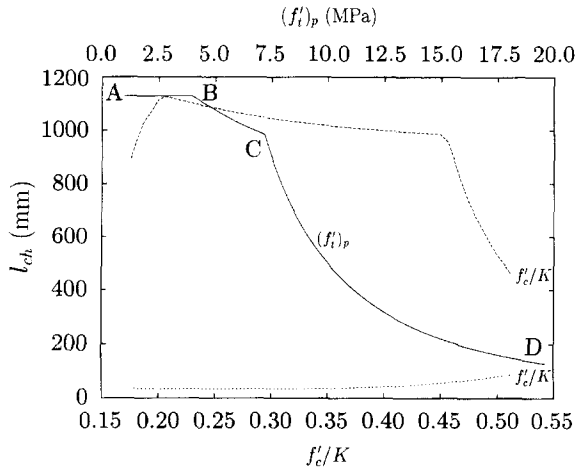

FIGURE 4. The optimum characteristic length versus direct tensile strength (solid; single-criterion optimization). Also shown are the optimum (long dash), maximum (long dash), and minimum (short dash) characteristic length versus relative compressive strength according to double-criterion optimization.

$$V = \frac{1 - 0.83(w/c)(\rho_c/\rho_w)}{1 + (w/c)(\rho_c/\rho_w)}$$

and

$$\Theta = 0.5\,[\eta_u \sqrt{1-V}(1-n) + \sqrt{\eta_u^2(1-V)(1-n)^2 + 4n}]$$

where η_u is a shape factor of an unhydrated cement particle. For $w/c > 1.2\rho_w/\rho_c$, the cement paste is regarded as a collection of capillary pores embedded in solid, hydrated cement gel. Now $n = 0$, $\Theta = \eta_k(1 - V)$ with η_k being a shape factor of a capillary pore and the volume fraction of capillary pores

$$V = \frac{w/c - 1.2\,\rho_w/\rho_c}{w/c + \rho_w/\rho_c}.$$

For mortar ($E = E_r$), $E_m = E_p$, n is the ratio of modulus of elasticity of the fine aggregate particles, E_f, to E_p and $V = V_f$. Moreover [15],

$$\Theta = \frac{1}{2}\left[q + \sqrt{q^2 + 4n[1 - \eta_f(1 - V_f) - n\eta_f(V_f - 1)]}\right] \tag{10}$$

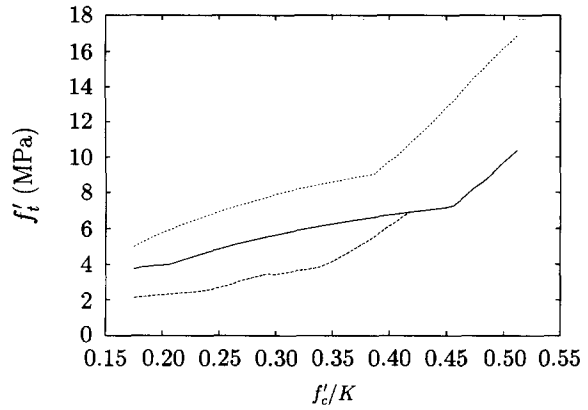

FIGURE 5. Relationship between direct tensile strength and relative compressive strength according to single- or double-criterion optimization (solid). Also shown are the maximum (short dash) and minimum (long dash) direct tensile strength versus relative compressive strength needed in double-criterion optimization.

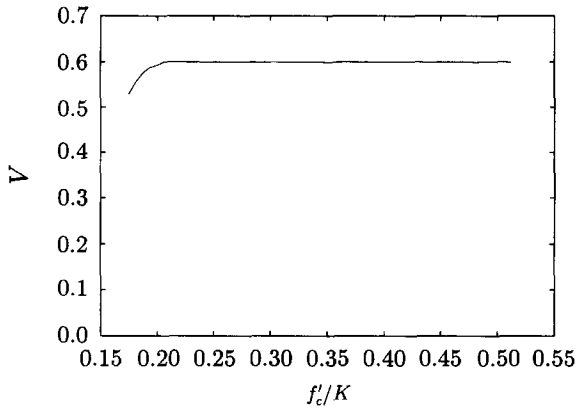

FIGURE 6. Optimum volume fractions of coarse and fine aggregate (which are equal $V_c = V_f = V$) versus relative compressive strength.

Here, $q = \eta_f(1 - V_f) + n\eta_f(V_f - 1)$ and

$$\eta_f = \frac{3A_f(1 + A_f)}{1 + A_f + 4A_f^2} \tag{11}$$

with A_f being the aspect ratio of the fine aggregate particles.

For concrete, $E_m = E_r$, $n = E_c/E_r(1 - \beta^{7.5/(5 + E_c/E_r)})$ with E_c the modulus of elasticity of the coarse aggregate particles. Θ is given by eq 10 in combination with eq 11 after replacing V_f with V_c, η_f with η_c, and A_f with A_c. V_c is the volume fraction of coarse aggregate, η_c is the shape factor of coarse aggregate particles, A_c is their aspect ratio, and β is the surface area of debonded coarse aggregate relative to its total surface area.

Finally, the variation in the uniaxial compressive strength, f'_c caused by the angularity, maximum size, volume fraction, and grading of the aggregate has been established empirically by Larrard and Tondat [6]. It can be written as

$$f_c' = K\left\{\frac{g}{g_f}\left[\left(\frac{1 - \lambda(d/g)^\kappa}{V_{agg}}\right)^{1/3} - 1\right]\right\}^{-0.16} \times \left(\frac{1 - V_{air}/(1 - V_{agg})}{1 + (w/c)(\rho_c/\rho_w)}\right)^2 \tag{12}$$

where $(\lambda,\kappa) = (0.39,0.22)$ or $(0.45,0.19)$ for rounded and sharp-edged angular aggregates, respectively, d is the maximum size of the bottom 10% in the aggregate grading curve, g_f is the maximum size of the fine aggregate, and K is an experimental constant depending upon g_f and other aggregate and cement parameters. Equation 12 appears to be valid for $V_{agg} \leq 0.99\ (1 - \lambda(d/g)^\kappa)$.

The following material parameters have been chosen for the calculations to follow: $\nu_m = \nu = 0.2$; $g_{av} = 0.25\ g$; $f_{t,a} = 10$ MPa; $h = 0.75$; $E_u = 75000$ MPa; $\eta_u = 1.0$: $\eta_k = 0.7$; $E_f = E_c = 65000$ MPa; $A_f = A_c = 1.0$; $\beta = 0.2$; $\eta = 10 \times 10^{-6}$ m; $\tau^* = 2.5$ MPa (cf. ref 17); $(\lambda,\kappa) = (0.39,0.22)$; $d = 0.01g$; $V_{air} = 0.02$, and $\rho_c = 3150$ kg/m^3. A Fuller-Thompson grading [18] has been assumed to determine d and g_{av}. Furthermore, the maximum aggregate size of the fine aggregate, g_f, is taken to be 4 mm.

Maximum Characteristic Length

The minimization of the concrete brittleness may be approached in the following two ways. First, l_{ch} is maximized ($-l_{ch}$ is minimized), thus leading to the following optimization problem:

$$\text{Minimize} - l_{ch}(w/c,g,V_c,V_f) = -\frac{EG_F}{f_t'^2} \tag{13}$$

by choosing w/c, g, V_c and V_f in such a way as to meet the micromechanical relations 1–11, a prescribed minimum tensile strength

$$f_t' \geq (f_t')p \tag{14}$$

and lower and upper bounds on the microstructural parameters (design variables)

$$\begin{aligned} 0.2 &\leq w/c \leq 0.45 \\ 0.004\text{ m} &\leq g \leq 0.032\text{ m} \\ 0.005 &\leq V_c, V_f \leq 0.6. \end{aligned} \tag{15}$$

TABLE 1. Mixes selected for studying the sensitivity of optimum characteristic length to changes in w/c, g, and V_c (=V_f)

Mix	w/c	g (mm)	$V_c = V_f$	E (GPa)	G_F (N/m)	f'_t (MPa)	l_{ch} (mm)	f'_c/K
I	0.428	32.00	0.60	46.56	432.21	4.25	1111.85	0.219
II	0.307	32.00	0.60	49.30	706.90	5.80	1035.91	0.312
III	0.230	32.00	0.60	50.82	906.40	6.80	997.38	0.406
IV	0.200	14.89	0.60	51.53	965.89	10.41	459.01	0.512

w/c = water/cement ratio; g = maximum size of aggregate; V_c = volume fraction of coarse aggregate; V_f = volume fraction of fine aggregate; E = modulus of elasticity; G_F = fracture energy; f'_t = direct tensile strength; l_{ch} = characteristic length; f'_c/K = relative compressive strength.

Secondly, l_{ch} and f'_t are maximized ($-l_{ch}$ and $-f'_t$ are minimized) simultaneously by introducing a preference function $F^{(\rho)}(x)$ [19]. This double-criterion optimization problem can be formulated as follows: For a prescribed f'_c,

$$\text{Minimize } F^{(\rho)}(x) = \left\{ \sum_{j=1}^{2} \left| \frac{f_j(x) - \min f_j}{\min f_j - \max f_j} \right|^p \right\}^{1/\rho} \tag{16}$$

with

$$\{x\} = \{w/c, g, V_c, V_f\}^T$$

$$f_1(x) = -l_{ch} \tag{17}$$

$$f_2(x) = -f'_t$$

by choosing $\{x\}$ in such a way as to meet the micromechanical relations 1–12 and the lower and upper bounds on microstructural parameters 15. T indicates transpose in 17.

These nonlinear mathematical programming problems were solved by the sequential linear programming (SLP) technique using the method of feasible directions combined with the golden section method. The SLP technique is available in a general purpose optimization package called the automated design synthesis (ADS) [20]. ADS requires an initial guess of values of the microstructural parameters in the vicinity of which an optimum is sought. These values were therefore systematically varied in order to ensure global optimal solutions.

The single-criterion optimization problem 13 has only one solution for all $(f'_t)_p < 4.00$ MPa or correspondingly all $f'_c/K < 0.212$. This optimal mix has w/c = 0.45, g = 32 mm, and $V_c = V_f = 0.6$, thus giving $f'_t = 4.00$ MPa, E = 45.91 GPa, G_F = 392.58 Nm/m^2, and l_{ch} = 1126.80 mm. Outside of this range of $(f'_t)_p$ that is, $f'_c/K \geq 0.212$, the mix attains the minimum permissible value of f'_t and V_c and V_f the upper bound of 0.6 while w/c and g vary, as shown in Figure 2. The resulting effective properties and the optimum characteristic length are displayed in Figures 3 and 4. The maximum l_{ch} is found to decrease with increasing f'_t. This result is in full accordance with available experimental data [21]. In region BC, a decreasing w/c (necessary for attaining the required f'_t) at constant (high) values of g, V_c, and V_f, causes E and G_F to increase. The maximum l_{ch} is therefore only slightly reduced. In region CD, however, as

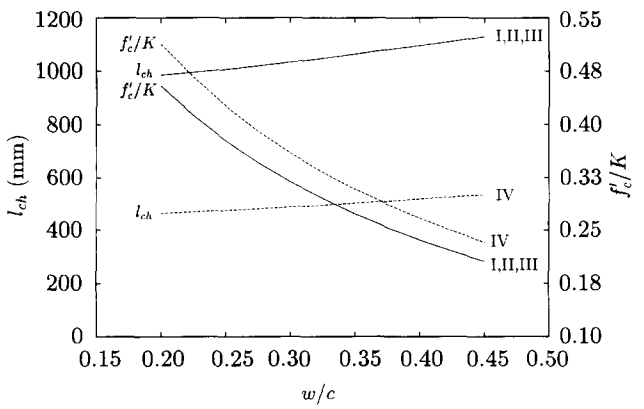

FIGURE 7. Sensitivity of optimum characteristic length and relative compressive strength to changes in water/cement ratio for mixes I, II, III, and IV of Table 1.

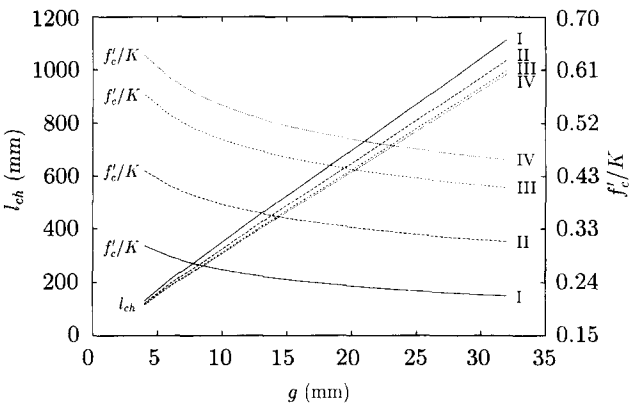

FIGURE 8. Sensitivity of optimum characteristic length and relative compressive strength to changes in maximum aggregate size for mixes I, II, III, and IV of Table 1.

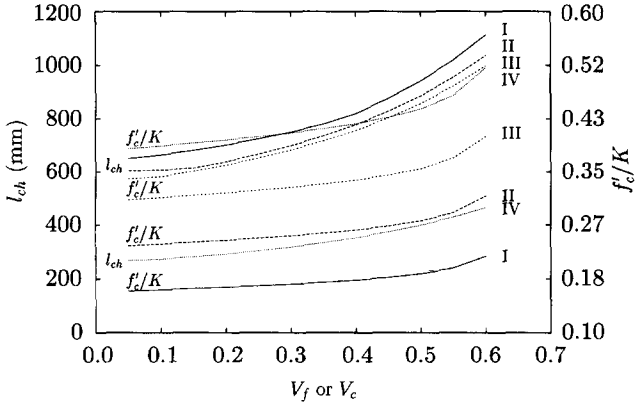

FIGURE 9. Sensitivity of optimum characteristic length and relative compressive strength to changes in volume fraction of coarse and fine aggregate for mixes I, II, III, and IV of Table 1.

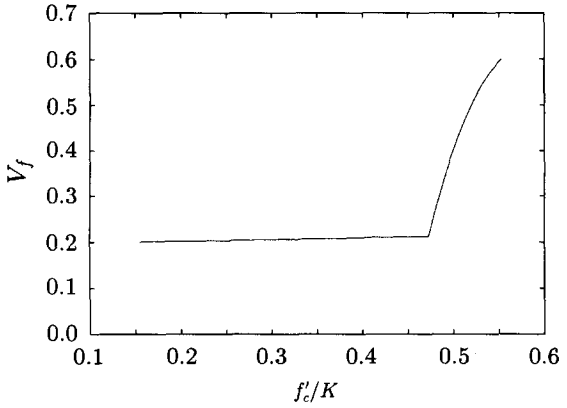

FIGURE 11. Optimum volume fraction of fine aggregate versus relative compressive strength for achieving minimum matrix brittleness.

w/c has reached its lower bound and g has started to decrease, E and G_F can no longer be increased, so that a pronounced reduction in maximum l_{ch} becomes inevitable. The optimum combination of mix parameters provides the relationship between f'_t and f'_c recorded in Figure 5 (solid line for $f'_c/K \geq 0.212$).

In the double-criterion optimization problem 16, $F^{(\rho)}(x)$ was found to be practically independent of ρ (≥ 8). For $\rho = 25$, the optimum values of the mix parameters are given in Figures 2 and 6 and the effective properties in Figures 3 and 5. The corresponding characteristic length is given in Figure 4. Also shown are the extreme values of f'_t and l_{ch} required in the preference function 16. Thus, the solution to the double-criterion optimization problem is identical to the solution of the single-criterion optimization problem (for $f'_c/K \geq 0.212$) and the solution obtained when maximizing l_{ch} for a prescribed f'_c.

The effect of a change in the value of a microstructural parameter on the optimum design may be assessed by varying that parameter while retaining all other microstructural parameters at their optimum values. For this purpose, the four optimum mixes given in Table 1 are considered.

Figure 7 represents a nearly linear relationship between l_{ch} and w/c, l_{ch} being rather insensitive to changes in w/c. As expected though, f'_c appears to be strongly affected by w/c, as illustrated in the same figure. Likewise, the variation of l_{ch} with g in Figure 8 is essentially linear but quite substantial, whereas g has little effect on f'_c, (cf. the same figure). The curves for f'_c and l_{ch} are (almost) identical for V_c and V_f (Figure 9) and indicate a considerable sensitivity near the optimum values. It thus seems that if strength requirements are changed, the new mix can be achieved by changing only w/c with practically no reduction in the value of l_{ch}. If, however, V_c and V_f are lowered, f'_c and l_{ch} may be considerably reduced.

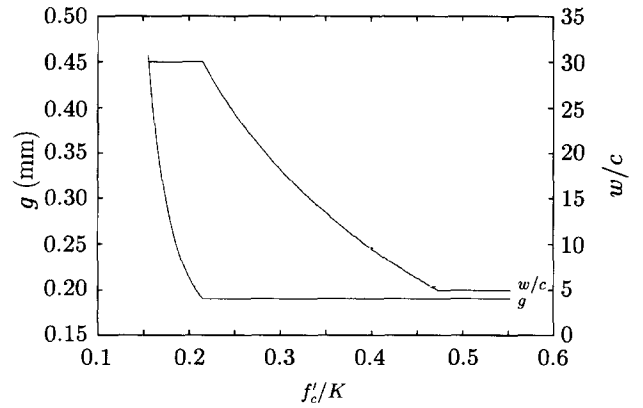

FIGURE 10. Optimum water/cement ratio and aggregate size versus relative compressive strength for achieving minimum matrix brittleness.

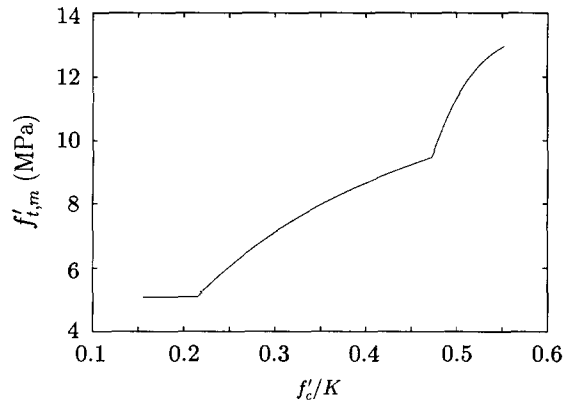

FIGURE 12. Direct tensile strength of the mortar versus relative compressive strength at minimum matrix brittleness.

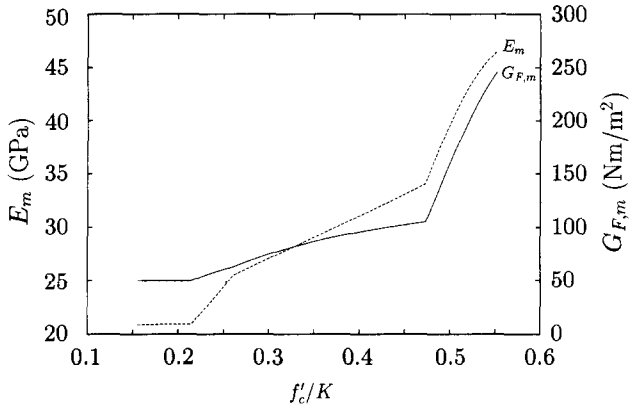

FIGURE 13. Optimum modulus of elasticity and fracture energy of the mortar versus relative compressive strength at minimum matrix brittleness.

Minimum Brittleness Number

Microcracking in bulk concrete, caused by the confinement exerted by coarse aggregate particles during shrinkage of the mortar, is controlled by the brittleness number [22]

$$B = \frac{g(f'_{t,m})^2}{E_m G_{F,m}}$$

where $f'_{t,m}$ is the direct tensile strength and $G_{F,m}$ is the fracture energy of the matrix, that is, mortar. Note that this brittleness number depends not only on the matrix properties but also on the maximum size of the coarse aggregate. Thus, to minimize the risk of microcracking, the brittleness number B should be as small as possible. Therefore, the following single-criterion optimization problem has been formulated: For a prescribed f'_c,

$$\text{Minimize } B\,(\text{w/c}, g, V_c, V_f) = \frac{g(f'_{t,m})^2}{E_m G_{F,m}} \qquad (18)$$

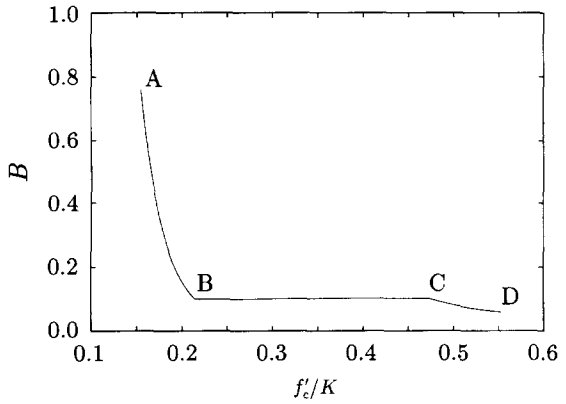

FIGURE 14. Minimum brittleness number of the matrix versus relative compressive strength.

TABLE 2. Mixes selected for studying the sensitivity of optimum matrix brittleness to changes in w/c, g, V_c, and V_f

Mix	w/c	g (mm)	V_f	V_c	B	f'_c/K
i	0.45	30.71	0.20	0.50	0.76	0.155
ii	0.45	4.02	0.20	0.50	0.10	0.215
iii	0.20	4.07	0.21	0.50	0.10	0.473
iv	0.20	4.08	0.60	0.50	0.06	0.553

w/c = water/cement ratio; g = maximum size of aggregate; V_c = volume fraction of coarse aggregate; V_f = volume fraction of fine aggregate; B = brittleness; f'_c/K = relative compressive strength.

by choosing w/c,g, and V_f in such a way as to meet the micromechanical relations 2–12, a prescribed $V_c = 0.5$, and lower and upper bounds on the microstructural parameters (design variables)

$$\begin{aligned} &0.2 \le \text{w/c} \le 0.45 \\ &0.004\ \text{m} \le g \le 0.032\ \text{m} \\ &0.2 \le V_f \le 0.6. \end{aligned} \qquad (19)$$

This problem was also solved by using ADS. The variations of w/c, g, and V_f are shown in Figures 10 and 11. The resulting properties of the matrix are given in Figures 12 and 13, and the optimum B is recorded in Figure 14. B is found generally to decrease with increasing compressive strength. In region AB, E_m, $f'_{t,m}$, and $G_{F,m}$ are constant due to constant values of w/c and V_f, but g drops to its lower bound thereby causing the decrease in B. In region BC, a decreasing w/c at constant g and V_f causes both E_m, $f'_{t,m}$, and $G_{F,m}$ to increase, with the result that B diminishes. In region CD, however, B is only slightly reduced because of an increasing V_f at constant w/c and g.

As above, four different optimum mixes (given in Table 2) are subjected to a sensitivity analysis. As seen

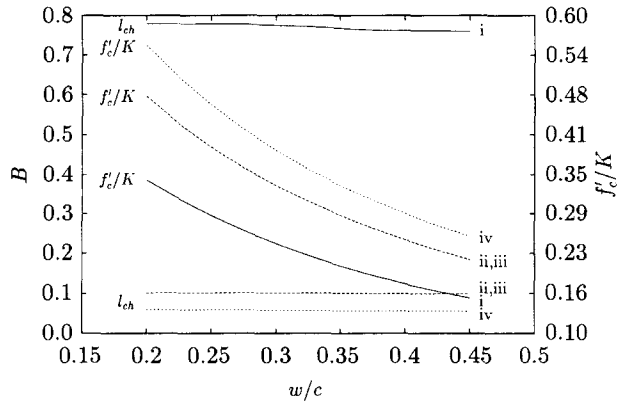

FIGURE 15. Sensitivity of minimum brittleness number and relative compressive strength to changes in water/cement ratio for mixes i, ii, iii, and iv of Table 2.

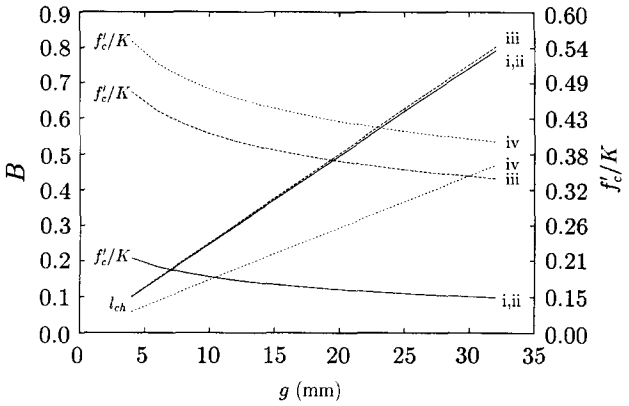

FIGURE 16. Sensitivity of minimum brittleness number and relative compressive strength to changes in maximum aggregate size for mixes i, ii, iii, and iv of Table 2.

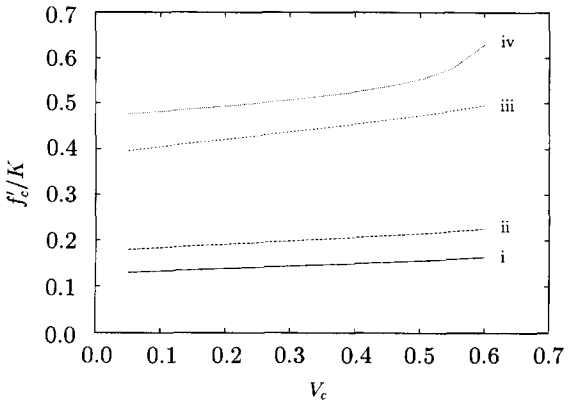

FIGURE 18. Sensitivity of relative compressive strength to changes in volume fraction of coarse aggregate for mixes i, ii, iii, and iv of Table 2.

from Figure 15, w/c has little effect on B but influences f'_c significantly. Furthermore, Figure 16 suggests that B depends nearly linearly on g and becomes less sensitive to changes in g when V_f attains a high value. Such a linear relationship also applies to B and V_f, as can be seen from Figure 17; a larger aggregate size produces concrete with a B that is more sensitive to changes in V_f. f'_c on the other hand, seems to be little influenced by changes in g, V_f, and V_c (Figures 16, 17, and 18).

Conclusions

The present study demonstrates that concrete mixes can be rigorously designed for optimal macroscopic properties. Of course, the accuracy of the designs depends on the validity of some of the empirical micromechanical relations. Notwithstanding this obvious limitation, it was found that mixes attain the same optimum combination of the microstructural parameters when employing either one of the following design criteria: (1) simultaneous maximum characteristic length and maximum tensile strength for a prescribed compressive strength; (2) maximum characteristic length for a prescribed compressive strength; and (3) maximum characteristic length for a prescribed (not too small, however) tensile strength. The maximum characteristic length is achieved for mixes with high volume fractions of coarse and fine aggregates, a high w/c ratio, and a large aggregate size. The most favorable way to attain the required compressive or direct tensile strength is by varying the w/c; the next most favorable way is by varying the maximum aggregate size. In addition, the study demonstrates that concrete mixes can be designed against microcracking on the basis of the brittleness number. Thus, mixes with a small aggregate size and high volume fraction of fine aggregate exhibit the largest resistance to microcracking. In this situation, the compressive strength is best controlled by the maximum aggregate size, followed by the w/c ratio, and the volume fraction of fine aggregate. Test mixes with the compositions in Table 1 are being prepared to verify the accuracy of the above optimum mixes. These results will be reported in a future communication. In summary, it seems advantageous to exploit the principles underlying the design of high performance concrete for the design of conventional concrete mixes of minimum brittleness.

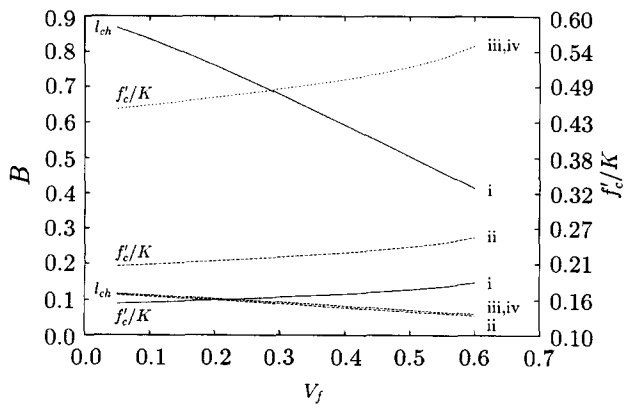

FIGURE 17. Sensitivity of minimum brittleness number and relative compressive strength to changes in volume fraction of fine aggregate for mixes i, ii, iii, and iv of Table 2.

References

1. Hillerborg, A. *Report TVBM-3004.* The Lund Institute of Technology: Sweden, 1977 (in Swedish).
2. Bache, H.H. In *Fracture Mechanics of Concrete Structures–From Theory to Applications,* Elfgren, L. Ed. Chapman & Hall: London, 1989; pp 202–207.
3. Bažant, Z.P. *ASCE Engng. Mech.* **1984,** *110,* 518–535.
4. Jenq, Y.; Shah, S.P. *ASCE Eng. Mech.* **1985,** *111,* 1227–1241.

5. Karihaloo, B.L. *Fracture Mechanics and Structural Concrete.* Longman Higher Education: UK, 1995; p 136.
6. Bache, H.H. In *Fracture Toughness and Fracture Energy of Concrete,* Wittmann, F.H., Ed. Elsevier Science Publishers: Amsterdam, 1986; pp 577–586.
7. Hillerborg, A. *Report TVBM-3005.* The Lund Institute of Technology: Sweden, 1978.
8. Karihaloo, B.L. *Fracture Mechanics and Structural Concrete.* Longman Higher Education: UK, 1995; p 166.
9. Huang, J.; Li, V.C. *Composites* **1989,** *20,* 370–378.
10. Karihaloo, B.L.; Fu, D.; Huang, S. *Mech. Mater.* **1991,** *11,* 123–134.
11. Li, V.C.; Huang, J. In *Micromechanics of Failure of Quasi-Brittle Materials,* Shah, S.P.; Swartz, S.E.; Barr, B., Eds. Elsevier Applied Science: London, 1990; pp 579–588.
12. Naus, D.J.; Lott, J.L. *ACI J.* **1969,** June, 481–489.
13. Ohgishi, S.; Ono, H.; Takatsu, M.; Tanahashi, I. In *Fracture Toughness and Fracture Energy of Concrete,* Wittmann, F.H., Ed. Elsevier Science Publishers: Amsterdam, 1986; pp 281–290.
14. Nielsen, L.F. *Tech. Rep. No. 208.* Build. Mat. Inst.: Tech. Univ. of Denmark, 1990 (in Danish).
15. Nielsen, L.F. *Tech. Rep. No. 287.* Build. Mat. Inst.: Tech. Univ. of Denmark, 1993 (in Danish).
16. Larrard, D. de; Tondat, P. *Mater. Struct.* **1993,** *26,* 505–516 (in French).
17. Ping, X.; Beaudoin, J.J. *Cem. Concr. Res.* **1992,** *22,* 23–26.
18. Mindess, S.; Young, J.F. *Concrete.* Prentice-Hall: Englewood Cliffs: NJ, 1981; p 239.
19. Wang, J.; Thomsen, N.B.; Karihaloo, B.L. In *Multidisciplinary Analysis and Optimization—Part 1,* Soebieski, J.; Borland, C.; Venkayya, V.; Berke, L.; Rozvany, G., Eds. AIAA, Washington, DC, 1994; pp 54–63.
20. Vanderplaats, G.N. *ADS—A FORTRAN Program for Automated Design Synthesis (version 2.00).* Engineering Design Optimization Inc.: Santa Barbara, CA, 1987; p 54.
21. Hilsdorf, H.K.; Brameshuber, W. *Int. J. Fracture* **1991,** *5,* 61–72.
22. Bache, H.H. *Nordic Conc. Res.* **1985,** *4,* 7–25.